

Ultrasonography of immature teratomas: 11 case reports

Z.Y. Shen^{1*}, B. Hu², G.L. Xia¹, K. Shen¹

¹Department of Radiology, Nantong Tumor Hospital, No. 30, North Tongyang Road, Nantong, Jiangsu, China 226361

²Department of Ultrasound in Medicine, Shanghai Institute of Ultrasound in Medicine, Shanghai Jiaotong University Affiliated Sixth People's Hospital, Shanghai, China 200233

ABSTRACT

► Original article

*** Corresponding author:**

Dr. Zhi-Yong Shen,

Fax: +86 513 86571201

E-mail: ntrgszy103@163.com

Received: June 2013

Accepted: Sept. 2013

Int. J. Radiat. Res., July 2014;
12(3): 203-209

Background: Ovarian immature teratoma is a very rare type of tumor associated with a high relapse rate and mortality. Correspondingly, early diagnosis is important for effective treatment. The goal of this study was to retrospectively analyze the ultrasound characteristics of 11 cases of immature teratomas. **Materials and Methods:** Between January 2002 and December 2010, 11 patients were diagnosed with pathologically confirmed immature teratomas. Patients enrolled in this study underwent a transabdominal ultrasound examination prior to surgery. Tumor size, shape, internal echo, calcification, cystic degeneration, and blood flow for each immature teratoma were analyzed. Levels of alpha fetal protein (α FP) were also evaluated. **Results:** The average tumor size was 8 cm (range, 4–13). Echo patterns obtained included mixed echo ($n = 7$), solid echo ($n = 2$), and cystic echo ($n = 2$). Coarse calcifications were detected in five cases, while blood flow signal was detected in one case, and ascites were detected in three cases. Only one case had elevated levels of α FP. **Conclusion:** Ultrasound imaging of immature teratomas detected large tumors that were predominantly involved mixed-echo masses, cystic degeneration, and coarse calcification on the cavity wall. In some cases, blood flow signal was detected in the mass and ascites were present in the abdominal cavity.

Keywords: Immature teratoma, ultrasound, calcification, alpha-fetal protein.

INTRODUCTION

Teratomas are common germ cell tumors that occur in females, and arise from totipotent primitive germ cells. Teratomas are composed of tissues derived from two or three germ cell layers⁽¹⁾, and are classified as mature teratomas if they contain differentiated tissues, or immature teratomas if they contain immature tissues. In the latter case, immature teratomas can contain varying amounts of neuroectodermal or blastemal tissues, and thus, are classified according to the amount of immature tissue present. This grading system was first intro-

duced by Norris *et al.*⁽²⁾, and was later modified by Gonzales-Crussi⁽³⁾. At the time of presentation, the symptoms most frequently reported were lower abdominal or pelvic pain, and an increase in abdominal girth.

Mature teratomas and immature teratomas have different treatment guidelines and prognoses. For example, mature teratomas are typically macroscopically resectable, while immature teratomas are treated with salpingo-oophorectomy, omentectomy, aortic lymph node dissection, appendectomy, and biopsy of the remaining ovary. In contrast with mature teratomas, immature teratomas are prone to

recurrence and peritoneal implants ⁽⁴⁾ and a rapid onset of death has been associated with implants, even with grade I implants ⁽⁵⁾. Therefore, an accurate diagnosis prior to surgery is of significant importance in order to identify the most effective treatment options and to establish an accurate prognosis. Currently, ultrasonography is the most commonly used diagnostic method for ovarian masses. Therefore, the aim of this study was to analyze the sonographic features of patients with immature teratomas.

MATERIALS AND METHODS

Patients

Between January 2002 and December 2010, 11 patients were diagnosed with immature teratomas and all the tumors were pathologically confirmed. The average patient age was 32 years (range, 12–62), and initial discomfort reported by patients was commonly associated with an unusual pelvic mass, abdominal distension, or abdominal pain and discomfort. Parents or guardians of these patients provided written informed consent prior to being enrolled in this retrospective study. This study was approved by the ethics committee of our institution. Clinical data, laboratory tests, imaging data, surgical notes, treatments, and results were obtained from each patient's medical records.

Methods

The initial diagnosis for all patients included a complete medical history, a physical examination, complete blood count, routine blood chemistry results, and serum levels of tumor markers, including alpha fetal protein (α FP).

Ultrasonography of pelvic masses was obtained using a Philips/ATL HDI 5000 (Universal Diagnostic Solutions, Oceanside, CA, USA) and PHILIPS IU22 (Philips Medical Systems, Bothell, WA, USA). At the time of imaging, patients had a full bladder and were maintained in a supine position in order to optimize imaging of the adnexal mass. Image analysis was performed by two independent individuals with more than ten years experience

reviewing sonograms and diagnosing ovarian masses.

Tumor size, shape, internal echo, presence of calcification, and cystic degeneration were detected for each immature teratoma using two-dimensional ultrasonography. The blood flow associated with each tumor was also analyzed using color flow imaging. The parameters of any blood signals obtained were further characterized by resistance index (RI) and pulse index (PI) values, which were recorded using pulse wave Doppler technology.

Levels of α FP in human serum or plasma samples were detected using enzyme-linked immunosorbent assays (ELISAs).

RESULTS

The clinical data and ultrasound characteristics of the 11 patients retrospectively analyzed in this study are listed in table 1. Representative ultrasonography images are also provided in figures 1-4.

Ovarian cysts or solid masses were detected during exploratory surgery. Although most tumors were maintained within a complete capsule, some tumors did not exhibit clear boundaries due to intestinal adhesions, while other tumors were associated with ascites. Additional observations of the tumors detected included: the presence of capsule hair, a grease-like substance, and the presence of some rough, partially gray papillary nodules. The capsule wall thickness also varied from 0.1–0.5 cm, and internal calcifications were observed. All histopathologic samples were evaluated by an experienced pathologist.

For 10/11 patients, their levels of α FP were found to be within the normal range (i.e., < 25 ng/ml), while the remaining patient had an α FP level of 127 ng/ml. According to the classification system previously established for teratomas, 7/11 (63.6%) cases in this series were classified as grade I, 2/11 (18.2%) cases were classified as grade II, and 2/11 (18.2%) cases were classified as grade III. Six tumors (cases 1, 2, 5–8) were correctly diagnosed pre-operatively, while the remaining five cases

were misdiagnosed as mature teratomas. Based on ultrasound imaging, mixed echo was detected in seven cases, coarse calcification was detected in five cases, ascites were detected in three cases, and affluent blood signal was detected in one case. In the latter case, the RI and PI values of the blood signal detected were 0.43 and 0.65, respectively.

DISCUSSION

Ovarian immature teratomas are a type of malignant germ cell tumor that represents less than one percent of all ovarian malignant tumors diagnosed. For treatment, imaging studies are critical. For example, computed tomography (CT) can reveal a contrast-enhanced mass consisting of both solid and cystic elements, as well as scattered point-shaped calcifications (6).

Compared with mature teratomas, immature teratomas are larger, less well-defined, have a prominent solid component, and are associated with foci of hemorrhage (7,8). In a previous study that evaluated immature teratomas using magnetic resonance (MR) imaging (9), all lesions that were detected appeared to be fat-containing tumors with solid components consisting of numerous cysts of various sizes. The solid tissues exhibited a wide variety of signal intensities on T2-weighted images. However, in most cases, ultrasound is the first method employed for imaging examinations. The characteristics of immature ovarian teratomas detected by ultrasound are reported less, in contrast to that of mature cystic teratomas, which are predominantly characterized by a well-defined ovarian tumor with a typical fat-fluid level and a round mass with a tuft of matted hair (6,10).

Table 1. Ultrasonography features and AFP results for the patients examined.

Case no.	Patient age (yr)	Sonography result	Tumor dimensions (cm ³)	AFP (ng/ml)	Pathology Results; Ultrasonography characteristics
1	28	CM	11 × 8 × 9	13	grade II; coarse calcification with acoustic shadow
2	24	SM and CM	9 × 9 × 7	19	grade III with SCC; blood flow signal within the mass, RI 0.43, PI 0.65
3	22	Mixed*	9 × 6 × 9	11	grade I; heterogeneous
4	17	CM	4 × 3 × 3	12	grade I; coarse calcification
5	58	Mixed	9 × 9 × 8	15	grade I; ascites
6	56	Mixed	12 × 11 × 12	127	grade I; coarse calcification, ascites
7	24	Mixed	8 × 7 × 9	18	grade I; coarse calcification with acoustic shadow, ascites
8	62	Mixed	5 × 4 × 5	21	grade III; coarse calcification
9	12	Mixed	4 × 4 × 5	19	grade I; no specialty
10	23	SM	8 × 7 × 8	11	grade II; heterogeneous
11	35	SM	5 × 3 × 5	21	Grade I; no specialty

*Mixed: Exhibited a prominent solid component with cystic elements; SM: solid mass; CM, cystic mass; IT, immature teratoma; RI: resistance index; PI: pulse index; SCC, squamous cell carcinoma.

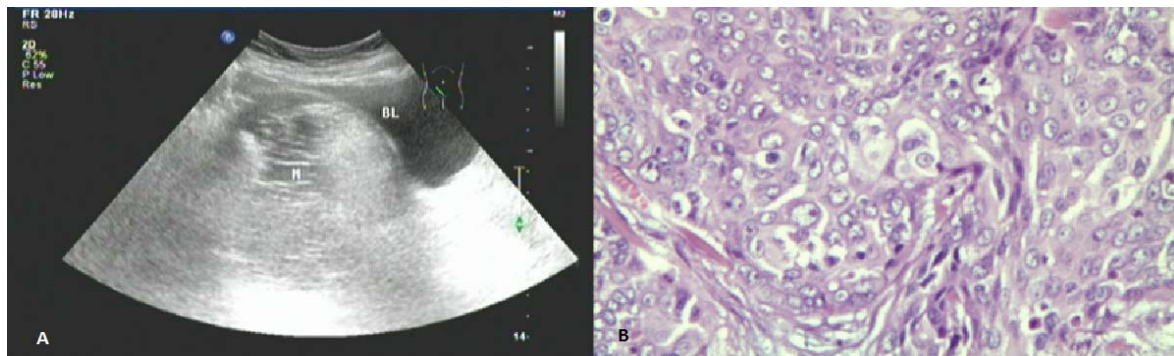


Figure 1. Ultrasonography (A) and pathological (B) analysis of a pelvic mass detected in a 24-year-old patient.

A patient experiencing abdominal distension underwent an ultrasound that detected a mixed mass with a diameter of 8 cm associated with coarse calcification in the thick tumor wall (magnification 200x).

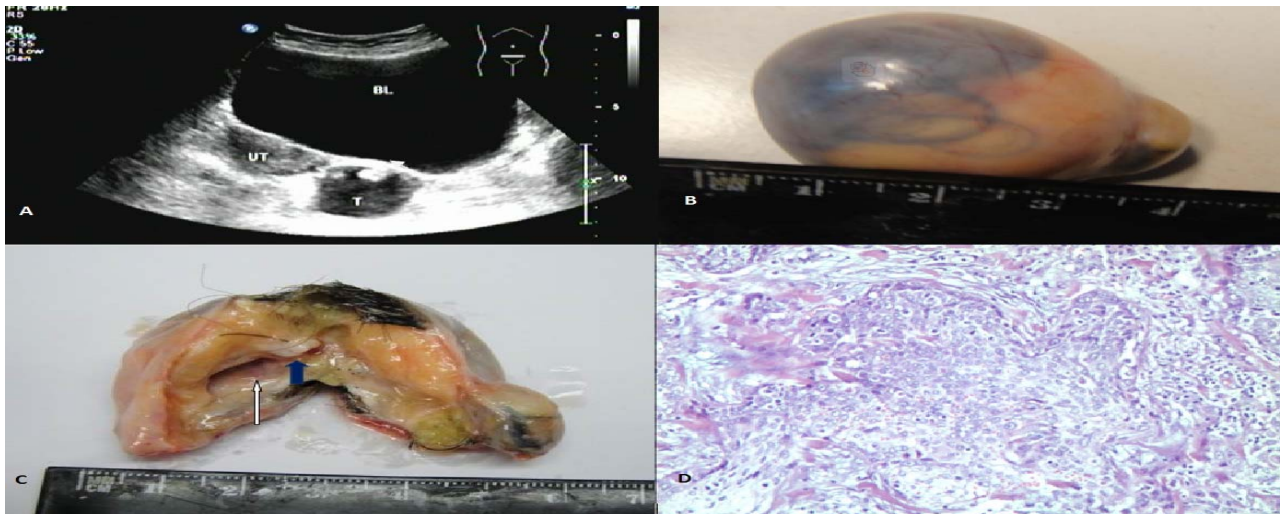


Figure 2. An ultrasound of a 17-year-old patient experiencing abdominal distension. A) A cyst with a heterogeneous internal echo and a diameter of 3.5 cm was detected (the white arrow indicates coarse calcification). B) Gross pathologic specimen of the tumor. C) Dissected specimen of the tumor; hair, necrotic hemorrhagic degeneration and coarse calcification (the blue arrow) were also observed. D) Immature neural tissue detected by hematoxylin/eosin staining (magnification, 100×).

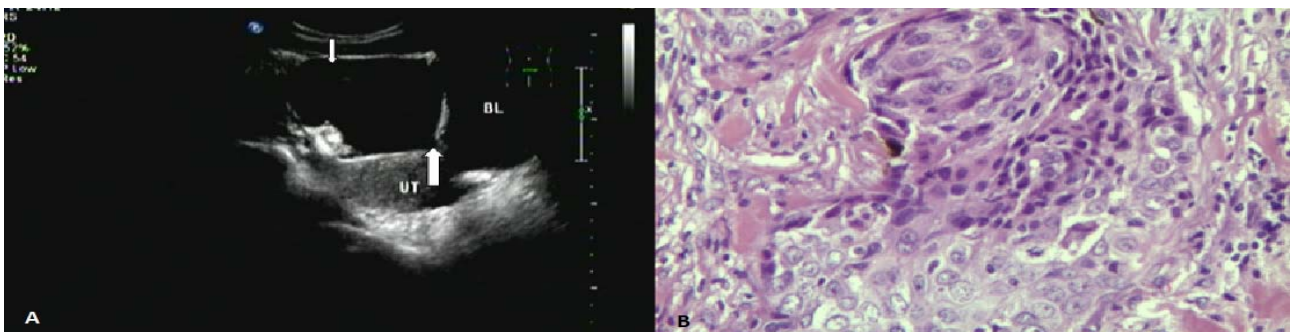


Figure 3. A) An ultrasound of a 28-year-old patient with a pelvic mass. Coarse calcifications adhered to the wall of a cyst (arrow) with a diameter of nine cm were detected. B) Immature neural tissue detected by hematoxylin/eosin staining (magnification, 200×).

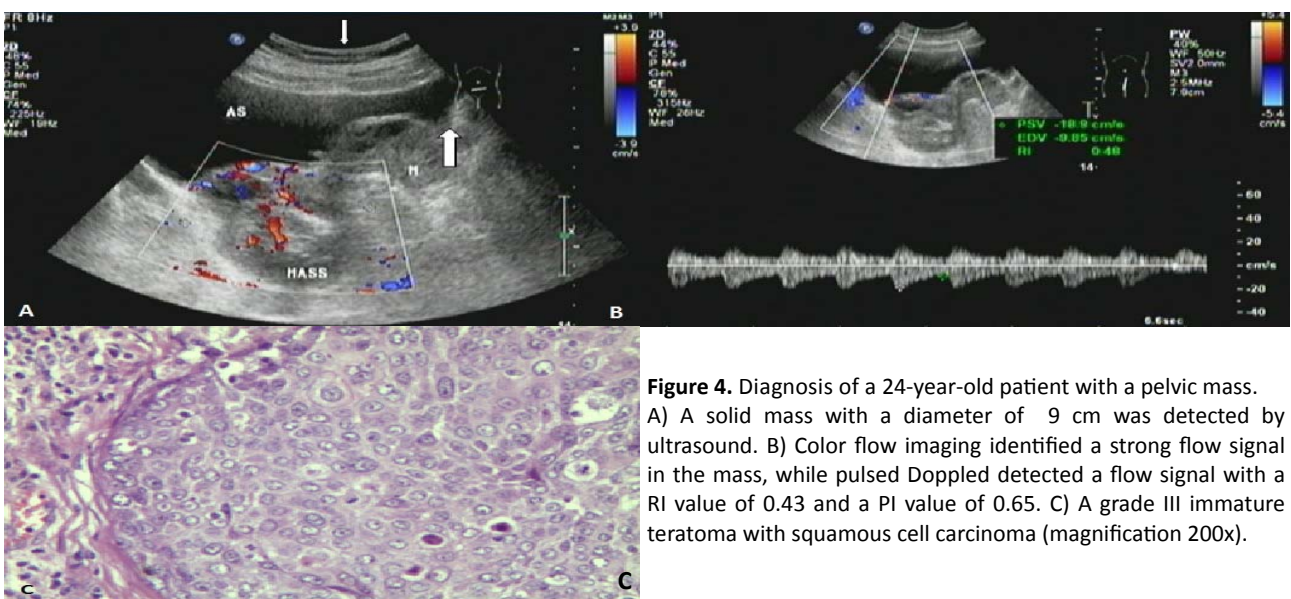


Figure 4. Diagnosis of a 24-year-old patient with a pelvic mass. A) A solid mass with a diameter of 9 cm was detected by ultrasound. B) Color flow imaging identified a strong flow signal in the mass, while pulsed Doppler detected a flow signal with a RI value of 0.43 and a PI value of 0.65. C) A grade III immature teratoma with squamous cell carcinoma (magnification 200×).

In the present study, the 11 cases of immature teratomas analyzed by ultrasonography were characterized by both the histologic subtype and the tumor components involved. Correspondingly, a mixed echo (n = 7) was detected for most of the immature teratomas evaluated, indicating the presence of multiple cystic and solid areas. Gross pathologic examination confirmed the presence of heterogeneous masses near the uterus and bladder, and these contained cystic, fatty, and calcified elements. Therefore, we report that immature teratomas contain a mixture of calcific, fatty, and fluid densities and are associated with a greater number of solid elements than mature teratomas.

The cystic aspect of immature teratomas can also represent regions of internal necrosis or hemorrhage (11), while small foci of fat can also be associated with immature teratomas. In the latter case, these foci of fat can represent rapidly growing tumors that frequently undergo a perforation of the tumor capsule containing them, thereby disrupting a well-defined tumor mass (12). Three of the eleven cases also had ascites in the abdominal cavity, indicating that the peritoneal area was infiltrated. In combination, these results are consistent with

another study of immature teratomas that used MR imaging (9).

Typically, an affluent blood flow signal is not detected in mature teratomas using ultrasound. However, malignant teratomas can manifest a blood flow signal when carcinomas are present. Abnormal blood flow can also be detected in stage I ovarian carcinomas by ultrasound (12). For tumor-induced vessels that are often dilated and saccular, they can also contain tumor cells within their endothelial lining (13). As a result, tumor microvasculature differs from that of normal tissue (13). Tumors can contain giant capillaries and arteriovenous shunts without intervening capillaries. As a result of these differences in tissue vasculature, an affluent blood flow signal can be detected within some malignant teratomas. In this series, only one tumor had affluent blood flow detected, and this is hypothesized to be due to the onset of necrosis of other tumors.

The other important ultrasound characteristics observed in this study was coarse calcification (n = 5). The pathologic equivalent of coarse calcification detected on ultrasound is the presence of bone or teeth, and if present, these tend to be located within so-called Rokitansky nodules (14,15). Coarse calcification can also contain immature elements such as

Table 2. Ultrasonography differences in the detection of mature versus immature teratomas.

	Mature cystic teratomas	Immature teratomas
Incidence rate	One of the most frequent ovarian tumors in female patients of reproductive age	Represent < 1% of ovarian teratomas and typically affect younger patients (< 20 y of age) (10)
Size	Average, 7 cm	Typically larger (14–25 cm)(25)
Border	Well-defined	Not always well-defined, frequently exhibit perforation of the capsule (26)
Gray scale ultrasound	Involve a cystic lesion with a densely echogenic tubercle (e.g., a Rokitansky nodule) projecting into the cyst lumen (10). Alternatively can be a diffusely or partially echogenic mass with the echogenic area usually demonstrating sound attenuation owing to sebaceous material and hair within the cyst cavity (28). Multiple thin, echogenic bands are caused by hair in the cyst cavity (6).	Appear solid, have a prominent solid component with cystic elements(27), or have a large, irregularly shaped solid component containing coarse calcifications (1)
	Calcification localized to the mural nodule (1)	Calcification typically scattered throughout the tumor (6)
	Fat intermixed with hair strands are echogenic and often attenuate the sound beam	Small foci of fat within the solid component can be difficult to recognize (6)
Color Doppler flow imaging	Seldom associated with intratumoral blood flow	Significant intratumoral blood flow detected (29)
	RI > 0.6; PI > 1 (29)	RI < 0.4; PI < 0.6 (29)

neuroectodermal tissue ^(11,16). Rarely is calcification observed on the cyst wall of a mature teratoma ⁽¹⁷⁾, however in the present study, coarse calcification was frequently associated with immature teratomas (figures 2-4). These results are consistent with those of Shin *et al.* where the presence of calcification facilitated a differential diagnosis ⁽¹⁸⁾.

α FP has previously been identified as a tumor marker associated with primary hepatic and embryonal germ-cell tumors, particularly yolk-sac tumors ⁽¹⁹⁾. Elevated levels of α FP have been detected in patients diagnosed with immature teratomas ^(20,21). In these cases, the neural component of the teratomas analyzed was hypothesized to be the source of α FP production ^(22,23). However, in the present study, only one case was associated with elevated α FP levels. Therefore, it would appear that ELISAs used to detect α FP do not provide sufficient sensitivity or specificity to be used independently for the diagnosis of teratomas. In contrast, ultrasonography in combination with color Doppler has been shown to be a useful preoperative test for the diagnosis of pelvic masses ⁽²⁴⁾, and the results of this study are consistent with this observation.

In conclusion, immature teratomas are large tumors that predominantly include mixed-echo masses which are often associated with cystic degeneration and coarse calcification. Furthermore, in some cases, blood flow signal is detected in the mass and ascites are present in the abdominal cavity. Overall, these observations were made from a small number of patients and treated lesions, and therefore, statistical analysis was not possible. Therefore, additional cases of immature teratomas are needed to confirm these results.

ACKNOWLEDGEMENTS

We sincerely thank Ming Feng Wu at the Nantong Tumor Hospital for providing important documents and valuable suggestions.

REFERENCES

1. Choudhary S, Fasih N, Mc Innes M, Marginean C (2009) Imaging of ovarian teratomas: appearances and complications. *J Med Imaging Radiat Oncol*, **53(5)**: 480-488.
2. Norris HJ, Zirkin HJ, Benson WL (1976) Immature teratoma of the ovary: a clinical and pathologic study of 58 cases. *Cancer*, **37(5)**: 2359-2372.
3. Gonzales Crussi (1982) Extragonadal teratoma. Atlas of tumor pathology, 2nd series fascicle 18. Armed Forces Inst of Pathology I, Washington, 44-129.
4. Alotaibi MO and Navarro OM (2010) Imaging of ovarian teratomas in children: a 9-year review. *Can Assoc Radiol J*, **61(1)**: 23-28.
5. Khoo SK, Jones IS, McKenna H (1978) Ovarian teratoma with peritoneal gliomatosis. *Aust N Z J Obstet Gynaecol*, **18(4)**: 277-280.
6. Outwater EK, Siegelman ES, Hunt JL (2001) Ovarian teratomas: tumor types and imaging characteristics. *Radiographics*, **21(2)**: 475-490.
7. Itani Y, Kawa M, Toyoda S, Yamagami K, Hiraoka K (2002) Growing teratoma syndrome after chemotherapy for a mixed germ cell tumor of the ovary. *J Obstet Gynaecol Res*, **28(3)**: 166-171.
8. Nimkin K, Gupta P, McCauley R, Gilchrist BF, Lessin MS (2004) The growing teratoma syndrome. *Pediatr Radiol*, **34(3)**: 259-262.
9. Yamaoka T, Togashi K, Koyama T, Fujiwara T, Higuchi T, Iwasa Y, Fujii S, Konishi J (2003). Immature teratoma of the ovary: correlation of MR imaging and pathologic findings. *Eur Radiol*, **13(2)**: 313-319.
10. Quinn SF, Erickson S, Black WC (1985) Cystic ovarian teratomas: The sonographic appearance of the dermoid plug. *Radiology*, **155(2)**: 477-478.
11. Brammer HM III, Buck JL, Hayes WS, Sheth S, Tavassoli FA (1990) Malignant germ cell tumors of the ovary: radiologic-pathologic correlation. *Radiographics*, **10(4)**: 715-724.
12. Fleischer AC, Cullinan JA, Peery CV, Jones JW III (1996) Early detection of ovarian carcinoma with transvaginal color Doppler ultrasound. *Am J Obstet Gynecol*, **174(1)**: 101-106.
13. Jain RK (1988) Determinants of tumor blood flow. *Cancer Res*, **48(10)**: 2641-2658.
14. Jung SE, Lee JM, Rha SE, Byun JY, Jung JI, Hahn ST (2002) CT and MRI imaging of ovarian tumors with emphasis on differential diagnosis. *Radiographics*, **22(6)**: 1305-1325.
15. Imaoka I, Wada A, Kaji Y, Hayashi T, Hayashi M, Matsuo M, Sugimura K. (2006) Developing an MR imaging strategy for diagnosis of ovarian masses. *Radiographics*, **26(5)**: 1431-1448.
16. Gallion H, Nagell JRV, Donaldson ES, Hanson MB, Powell DF (1983) Immature teratoma of the ovary. *Am J Obstet Gynecol*, **146(4)**: 361-365.
17. Fridman AC, Pyatt RS, Hartmann DS (1982) CT of benign cystic teratomas. *AJR Am J Roentgenol*, **138(4)**: 659-665.
18. Shin NY, Kim MJ, Chung JJ, Chung YE, Choi JY, Park YN. (2010) The differential imaging features of fat-containing tumors

- in the peritoneal cavity and retroperitoneum: the radiologic-pathologic correlation. *Korean J Radiol*, **11(3)**: 333-345.
19. El-Bahrawy M (2010) Alpha-fetoprotein-producing non-germ cell tumours of the female genital tract. *Eur J Cancer*, **46(8)**: 1317-1322.
 20. Pauniah SL, Tatti O, Lahdenne P, Lindahl H, Pakarinen M, Rintala R, Heikinheimo M (2010) Tumor markers AFP, CA 125, and CA 19-9 in the long-term follow-up of sacrococcygeal teratomas in infancy and childhood. *Tumour Biol*, **31(4)**: 261-265.
 21. Hsieh YL and Liu CS (2009) Progression from an immature teratoma with miliary gliomatosis peritonei to growing teratoma syndrome with nodular gliomatosis peritonei. *Pediatr Neonatol*, **50(2)**: 78-81.
 22. Billmire DF and Grosfeld JL (1986) Teratomas in childhood: analysis of 142 cases. *J Pediatr Surg*, **21(6)**: 548-551.
 23. Ohtsuka M, Satoh H, Inoue M, Yazawa T, Yamashita YT, Sekizawa K, Hasegawa S. (2000) Disseminated metastasis of neuroblastomatous component in immature mediastinal teratoma: a case report. *Anticancer Res*, **20(1B)**: 527-530.
 24. Medeiros LR, Rosa DD, da Rosa MI, Bozzetti MC (2009) Accuracy of ultrasonography with color Doppler in ovarian tumor: a systematic quantitative review. *Int J Gynecol Cancer*, **19(2)**: 230-236.
 25. Caldas C, Sitzmann J, Trimble CL, McGuire WP III (1992) Synchronous mature teratomas of the ovary and liver: a case presenting 11 years following chemotherapy for immature teratoma. *Gynecol Oncol*, **47(3)**: 385-390.
 26. Talerman A (1997) Germ cell tumors of the ovary. *Curr Opin Obstet Gynecol*, **9(1)**: 44-47.
 27. Malkasian GD, Symmonds GD, Dockerty MB (1965) Malignant ovarian teratomas. *Obstet Gynecol*, **25**:810-814.
 28. Patel MD, Feldstein VA, Lipson SD, Chen DC, Filly RA (1998) Cystic teratomas of the ovary: diagnostic value of sonography. *AJR Am J Roentgenol*, **171(4)**: 1061-1065.
 29. Emoto M, Obama H, Horiuchi S, Miyakawa T, Kawarabayashi T (2000) Transvaginal color Doppler ultrasonic characterization of benign and malignant ovarian cystic teratomas and comparison with serum squamous cell carcinoma antigen. *Cancer*, **88(10)**: 2298-2304.

